Design of wind farm layout with non-uniform turbines using fitness difference based BBO

Jagdish Chand Bansal*, Pushpa Farswan†
South Asian University, New Delhi, India

Atulya K. Nagar‡
Liverpool Hope University, UK

February 26, 2018

Abstract

Biogeography-based optimization (BBO) is an emerging meta-heuristic algorithm. BBO is inspired from the migration of species from one island to another. This study presents the solution of the wind farm layout optimization problem with wind turbines having non-uniform hub heights and rotor radii using BBO and an improved version of BBO. This study proposes an improved version of BBO, Fitness Difference Based BBO (FD-BBO). FD-BBO is obtained by incorporating the concept of fitness differences in original BBO. First, in order to justify the superiority of FD-BBO over BBO, it is tested over 15 standard test problems of optimization. The numerical results of FD-BBO are compared with the original version of BBO and an advanced version of BBO, Blended BBO (BBBO). Through graphical and statistical analyses, FD-BBO is established to be an efficient and accurate algorithm. The BBO, BBBO and FD-BBO are than applied to solve the wind farm layout optimization problem. In the considered problem, not only the location of the wind turbines but hub heights and rotor radii are also taken as decision variables. Two cases of the problems are dealt: 26 turbines in the farm size of $2000m \times 2000m$ and 30 turbines in the farm size of $2000m \times 2000m$. Numerical results are compared with earlier published results and that of original BBO and Blended BBO. It is found that FD-BBO is the better approach to solving the problem under consideration.

Keywords

Wind farm layout, Wind turbine, Hub height, Rotor radius, Biogeography-based optimization, Fitness difference

1 Introduction

Now a days energy is very important part of our necessity. Energy is becoming our inevitability in daily routine. Availability of energy is a very critical issue for future needs. Technologies are promoting renewable energy. Wind energy has been the fastest growing source of renewable energy from the twentieth century. Maximization of wind energy is the most promising area of research in the field of renewable energy. In this study, we have considered wind energy system for maximization of energy production with the help of non-conventional optimization techniques. The power output of wind farm depends on the locations, hub heights and rotor radii of wind turbines. There are lots of studies done in these directions. The power output of wind farm is sensitive to other parameters also. But in this study, we have considered only three parameters of wind turbines such as wind turbine location, hub height and rotor radius which affects the energy production significantly. The main concern of the study

*jcbansal@gmail.com
†pushpafarswan6@gmail.com
‡nagara@hope.ac.uk

is to increase the power output of wind farm. In this regard, we are maximizing the energy output with three parameters of wind turbines. Many non-conventional approaches have been applied to the problems related to wind energy systems.

Mosetti et al. [1] used a non-conventional optimization algorithm (genetic algorithms) to extract maximum energy output corresponding to the minimum installation cost. They used 100 square cells as possible locations for the wind turbines. Grady et al. [2] also used a genetic algorithms to find the optimal position of wind turbines as well as the limit of the maximum number of turbines for the considered wind farm of size ($2km \times 2km$). Marmidis et al. [3] introduce Monte Carlo simulation in wind park optimization system to produce maximum energy with minimum installation cost. They compared their findings with earlier studies [1, 2]. Acero et al. [4] maximize the energy production by optimizing the placement of wind turbines on a straight line. They considered Jensen's wake model [5] and two optimization techniques (simulated annealing and genetic algorithms) used in their study. Mittal [6] developed a code for wind farm layout optimization using the genetic algorithm (WFLOG) to finding optimal position of wind turbines in the given wind farm, so that cost per power minimizes. In that study, considered cell size was $1m \times 1m$ rather than $200m \times 200m$ used in [1, 2]. Gonzalez et al. [7] used a more realistic integral wind farm cost model that is based on a real life cycle cost approach. They introduced evolution approach to optimize the wind farm layout. Chowdhury et al. [8] proposed a new methodology the unrestricted wind farm layout optimization (UWFLO), to find optimal layout of the wind farm along with the selection of wind turbines corresponding to several rotor diameters. They used particle swarm optimization technique in their proposed study. Chen et al. [9] applied genetic algorithms to find the optimal layout of the wind farm corresponding to two possible hub heights ($50m$ and $78m$) of wind turbines. Park et al. [10] incorporated sequential convex programming for maximizing power production of the wind farm. Chen et al. [11] introduced wind turbine layout optimization corresponding to multiple hub heights of the wind turbines using the greedy algorithm. Bansal et al. [12] proposed optimal wind farm layout using BBO algorithm. They also recommended the maximum number of wind turbines which can be accommodated in a wind farm of given size. Recently S. Rehman et al. proposed a variant of cuckoo search algorithm [13] by incorporating a heuristic-based seed solution for better wind farm layout design [14]. In [15], Vasel et al. explored hub height optimization in their study and recommended multiple hub height turbines to maximize energy annually.

In this study, we apply a modified BBO algorithm to find wind farm layout with non-uniform hub heights and rotor radii. Biogeography-based optimization (BBO) is a nature inspired meta-heuristic algorithm based on the migration of species among islands. BBO is recently introduced by Dan Simon in 2008 [16]. BBO is popular among researchers due to few control parameter and its efficiency. This motivated the researchers to develop BBO algorithm to solve complex real-world optimization problems. There have been significant development in BBO algorithm by improving and introducing new operators. Some improved migration [17, 18, 19, 20, 21, 22, 23], mutation [24, 25] and new operators [26, 27] are developed earlier. Ma et al. [17] proposed Blended BBO (BBBO) to handle constrained optimization problems. In BBBO, information is blended, i.e. immigrating island accepts the information (feature) from itself and emigrating island. Feng et al. [18] proposed an improved BBO (IBBO) by improving migration operator. Xiong et al. [19] proposed polyphyletic BBO (POLBBO) by introducing polyphyletic migration operator. Wang et al. [20] introduced the krill herd algorithm with new migration operator in BBO. Lohakare et al. [24] proposed a memetic algorithm named as aBBOmDE. In aBBOmDE, the convergence speed of BBO is accelerated by incorporating the mutation operator of DE. Simon et al. [26] proposed Linearized BBO (LBBO) to solving non-separable problems. In LBBO, a local search operator is introduced with periodic re-initialization to make the algorithm appropriate for global optimization in a continuous search space. Bansal et al. [27] proposed DisruptBBO (DBBO) by introducing new operator in BBO algorithm to improve its exploration and exploitation capability. Although, various variants of BBO have developed and most of the developments are related to the tuning of migration and mutation operators of BBO algorithm. However, this study gives new insights into developing the performance of BBO algorithm. In this study, we introduce the fitness difference strategy in BBO algorithm (given in section 3). The so developed Fitness Difference based BBO (FD-BBO) algorithm and proposed approach is then applied to solve wind energy optimization problem with non uniform wind turbines. As a future study, different nature inspired algorithm such as artificial bee colony [28], spider monkey optimization [29], water Cycle Algorithm [30] and particle swarm optimization [31] etc. can also be applied to solve wind farm layout optimization problem with non uniform

turbines.
Rest of the paper is organized as follows: Section 2 describes the basic BBO algorithm. The discussion of proposed Fitness Difference based BBO (FD-BBO) approach and the numerical experiments are given in section 3. In section 4, the description of wind farm layout optimization problem is given and this section also discusses the various results of wind farm layout solved using proposed BBO, basic BBO and BBBO. The paper is concluded in section 5.

2 Biogeography-Based Optimization

Biogeography is the study of geographical distribution of biological organism in geographic space. The mathematical model of biogeography is modeled by Robert Mac Arther and Edward Wilson. The model describes the migration of species from one island to another island, the extinction of existing species from the island and the arrival of new species in the island [32]. However, very recently a new population-based evolutionary technique has been proposed based on biogeography theory and it has been named as the Biogeography-based optimization (BBO) [16]. BBO is a technique inspired by migration of species within islands [32]. BBO procedure is the design of population-based optimization procedure that can be potentially applied to optimize many engineering optimization problems. In biogeography model, the fitness of a geographical area (or island, or habitat) is evaluated by habitat suitability index (called HSI). Higher or lower HSI habitats correspond to higher or lower suitability of species to survive in the islands. Therefore, high HSI and low HSI corresponds to the large and small number of species, respectively. The variables that characterize the habitability are called suitability index variables ($SIVs$) e.g. rainfall, temperature, vegetation etc. The migration of species from one habitat to another habitat is mainly governed by two parameters, immigration rate (λ) and emigration rate (μ). Where λ and μ are the functions of the number of species in a habitat. Fig. 1 shows the relation between the number of species and migration rates (λ and μ) [32, 16]. In model given in Fig. 1 shows a special case i.e. maximum immigration rate (I) and maximum emigration rate (E) are equal. From the model given in Fig. 1, it is clear that if there are zero species on the habitat, then maximum immigration to habitat will occur and if there are the maximum number of species (S_{max}) on the habitat, then maximum emigration from habitat will happen. Therefore, for the small number of species, there is more possibility of immigration of species from another habitat and less possibility of emigration of species from this habitat to another habitat. In the equilibrium state, immigration and emigration of species are same and in this state, the number of species is denoted by S_0.

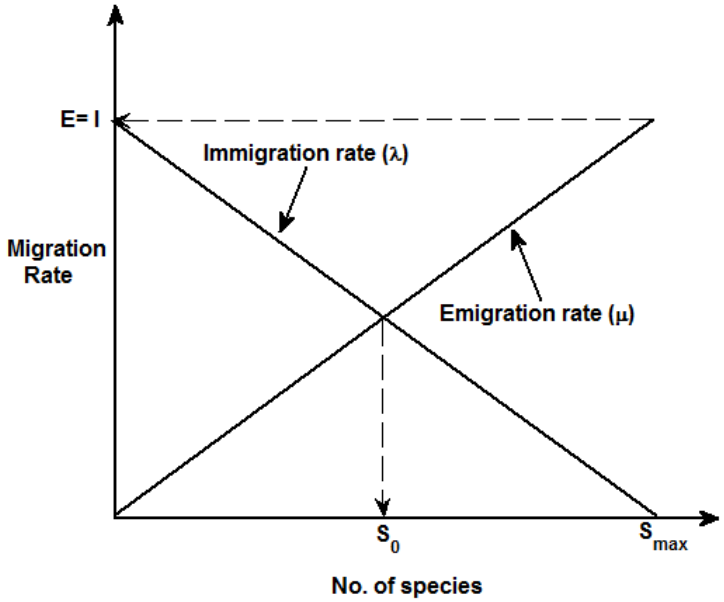

Figure 1: Relation between number of species and migration rate [16]

Let us assume that $P_s(t)$ is the probability given for s species in the habitat at any time t.

$$P_s(t+\Delta t) = P_s(t)(1-\lambda_s\Delta t - \mu_s\Delta t) + P_{s-1}\lambda_{s-1}\Delta t + P_{s+1}\mu_{s+1}\Delta t \tag{1}$$

Where λ_s and μ_s stand for immigration and emigration rate, respectively when there are s species in the habitat.
From the Eq. 1, one of the following conditions must hold for s species in the habitat at time $t+\Delta\ t$.

1. If there were s species in the habitat at time t, then there is no immigration and emigration occurred between time t and $t+\Delta t$.

2. If there were $(s-1)$ species in the habitat at time t, then only one species immigrated between time t and $t+\Delta t$.

3. If there were $(s+1)$ species in the habitat at time t, then only one species emigrated between time t and $t+\Delta\ t$.

For ignoring the probability of more than one immigration or emigration, Δt is considered very small. Letting $\Delta t \longrightarrow 0$

$$\dot{P}_s = \begin{cases} -(\lambda_s+\mu_s)P_s + \mu_{s+1}P_{s+1}, & s=0 \\ -(\lambda_s+\mu_s)P_s + \lambda_{s-1}P_{s-1} + \mu_{s+1}P_{s+1}, & 1 \le s \le s_{max}-1 \\ -(\lambda_s+\mu_s)P_s + \lambda_{s-1}P_{s-1}, & s = s_{max} \end{cases} \tag{2}$$

Let us define λ_n and μ_n are maximum immigration and emigration rate. S_{max} is the maximum possible number of species in the habitat. Therefore, we can obtain a matrix relation executing the dynamic equations of the probabilities of the number of species in the habitat.

$$\begin{bmatrix} \dot{P}_0 \\ \dot{P}_1 \\ \vdots \\ \vdots \\ \dot{P}_{S_{max}} \end{bmatrix} = \begin{bmatrix} -(\lambda_0+\mu_0) & \mu_1 & 0 & \cdots & 0 \\ \lambda_0 & -(\lambda_1+\mu_1) & \mu_2 & \cdots & \vdots \\ \vdots & \ddots & \ddots & \ddots & \vdots \\ \vdots & \ddots & \lambda_{n-2} & -(\lambda_{n-1}+\mu_{n-1}) & \mu_n \\ 0 & \cdots & 0 & \lambda_{n-1} & -(\lambda_n+\mu_n) \end{bmatrix} \begin{bmatrix} P_0 \\ P_1 \\ \vdots \\ \vdots \\ P_{S_{max}} \end{bmatrix} \tag{3}$$

BBO procedure is based on two simple biogeography concepts migration and mutation. BBO algorithm is designed as each habitat is a $m \times 1$ potential solution vector. Where m is the number of $SIVs$ (features) in each habitat. The number of species depends on the features quality i.e. habitats with good features have the higher number of species and habitat with worse features have less number of species. HSI of each habitat corresponds to fitness function of population-based algorithms. Habitat with the highest or lowest HSI reveals the best or the worst candidate for the optimum solution among all candidates. We considered N_p number of habitats in the ecosystem i.e. the total number of candidates (or individuals or population size) is N_p. In the basic BBO algorithm, migration rates (immigration and emigration rates) are calculated using the following formulae:

$$\lambda_i = I\left(1 - \frac{k_i}{n}\right) \tag{4}$$

$$\mu_i = E\left(\frac{k_i}{n}\right) \tag{5}$$

Here λ_i and μ_i are immigration and emigration rates of the i^{th} candidate (habitat). n is the maximum possible number of species that a habitat can support. k_i is the fitness rank of i^{th} habitat after sorting the habitat based on fitness value. Therefore, the worst solution rank is taken as 1 and the best solution rank is taken as n. In BBO, elitism saves the best solution in the population. In elitism approach, features of the best individuals are saved which has the best solution in BBO process. Elitism can be implemented by setting λ=0 for l best habitats. Here l is elitism parameter selected by the user. Algorithm 1 describes the pseudo code of BBO.

Algorithm 1 Biogeography-based optimization algorithm

```
Initialize the population.
Sort the population in descending order of fitnesses.
Calculate λ_i and μ_e ∀ i, e ∈ 1, 2, 3, ...., N_p.
for Generation index = 1 to Maximum generation do
  \\ Apply the migration operator
  for i = 1 to N_p do
    Select habitat H_i according to λ_i.
    if rand(0, 1) < λ_i then
      for e = 1 to N_p do
        Select habitat H_e according to μ_e.
        Replace the selected SIV of H_i by randomly selected SIV of H_e.
      end for
    end if
  end for
  \\ Apply the mutation operator
  for i = 1 to N_p do
    Compute mutation probability m(S).
    if rand(0, 1) < m(S) then
      Replace H_i(SIV) with randomly generated SIV.
    end if
  end for
  Sort the population in descending order of fitnesses.
  \\ Apply elitism
  Save some (elitism size) best solution of previous generation in current solution.
  Stop, if termination criterion is satisfied.
end for
```

Two crucial operators migration and mutation in BBO are designed to exploitation towards the solution and exploration in the whole search space, respectively. In both procedure (migration and mutation) new candidate solutions evolve. This procedure of evolving the habitats to the migration

procedure, followed by the mutation procedure, is continued to next generation until the stopping criterion is satisfied. The stopping criterion can be the maximum number of generations or obtaining the acceptable solution. The basic concept of migration operator is to probabilistically share the information within habitats using their migration rates (λ and μ). The migration operator is same as the crossover operator of the evolutionary algorithm and is responsible for sharing the feature among candidate solutions for modifying fitness. In the migration procedure, immigrating habitat is selected according to the probability of immigration rate and emigrating habitat is selected according to the probability of emigration rate of habitats. Then it is probabilistically decided that which of the SIV of immigrating habitat needs to be modified. Once the SIV is selected, algorithm replaces that SIV by emigrating habitat's SIV. The other important operator is the mutation which is occurred by random events. Mutation operator maintains the diversity of population in BBO procedure. Analysis of Fig. 1 reveals that highest HSI solution and lowest HSI solution have very low probabilities while medium HSI solutions have the relatively high probability to exist as a solution. Therefore, mutation process gives same chance to improve low HSI solutions as to high HSI solutions. The mutation rate $mut(i)$ is expressed as:

$$mut(i) = m_{max}\left(1 - \frac{P_i}{P_{max}}\right) \tag{6}$$

Where m_{max} is the user defined parameter and $P_{max} = max\{P_i\}$; i=1, 2,...., N_p.
The next section proposes a modified BBO named as Fitness difference Based BBO (FD-BBO).

3 Proposed Fitness difference Based BBO

3.1 Motivation

There is always a scope for modification in any nature-inspired optimization algorithm. Thus is also not an exception. In basic BBO, there is no criterion for an individual placing back to their previous position if it is moving apart from the optimal position. To get rid of this lacuna fitness difference based sorting strategy followed by selection procedure is proposed to be incorporated with BBO is applied to BBO algorithm. Selection procedure pulls back the solution to it's previous best position if the current solution is not better than previous. The fitness difference strategy is more efficient than the basic strategy of BBO algorithm. In the basic BBO, sorting is carried out based on the fitness of individuals but in fitness difference strategy sorting is based on fitness differences (for details see section 3.2). In this study, proposed strategy refines good solutions early and enhances the algorithm's efficiency.

3.2 Fitness difference strategy

Fitness difference strategy is based on absolute fitness difference between any two individuals. For a minimization problem, less fitness difference is considered as high rank and large fitness difference is considered as low rank. So the population is sorted in ascending order of fitness differences. The proposed strategy is applied after the population update using original BBO operators, migration and mutation. Also, the strategy is applied only if the following condition is satisfied:

$$\mid fit^{old}_{gbest} - fit^{new}_{gbest} \mid \leq fit^{new}_{gbest} \times 0.01 \tag{7}$$

Here fit^{old}_{gbest} is the fitness of the best individual before applying BBO operators, while fit^{new}_{gbest} is the fitness of the best individual after applying BBO operators. In the fitness difference based strategy, the sorting is carried out based on absolute difference $\mid fit^{old}_i - fit^{new}_i \mid$, where fit^{old}_i and fit^{new}_i are the fitnesses of i^{th} individual before applying BBO operators and after applying BBO operators, respectively. This sorting strategy performs better than sorting strategy of original BBO if it follows selection procedure given in section 3.3.

3.3 Selection operator

Selection operator is based on fitness values. After fitness difference strategy, since we have three populations: before applying BBO operators; after applying BBO operators and after applying fitness

difference strategy. Let us call these populations as grand parents, parents and offsprings, respectively. Selection operator saves the better quality solution in each generation. It selects the best individual, between grandparent and the offspring of current generation individual. Selection operator refines the better solutions. This operator is applied between grandparents and offsprings. If the offspring's fitness value ($fit_{current}x_i(Generation\ index)$) is better than grandparent's fitness value ($fit_{initial}x_{i_0}$), then the offspring, i.e. current solution will proceed to the next generation otherwise, the grandparent, i.e. initial solution (x_{i_0}) will proceed for improvement in the next generation.

$$x_i(Generation\ index+1) = \begin{cases} x_i(Generation\ index), \\ \quad if\ fit_{current}x_i(Generation\ index) > fit_{initial}x_{i_0} \\ x_{i_0}, \quad otherwise \end{cases} \tag{8}$$

Selection operator retains the good individuals of the previous generation who are moving apart from the optimal solution. Due to selection operator, a better individual always selected for the next generation.

3.4 BBO with Fitness difference strategy

In order to retain good solution in any generation, the fitness difference based strategy is applied to BBO algorithm. The main objective of the incorporation of fitness difference strategy is to refine the better solutions in each generation. In this study, a fitness difference based sorting criterion (section 3.2) followed by selection procedure (section 3.3), has been incorporated into the basic version of BBO. Thus, fitness difference strategy and selection operator defined in (7) and (8), respectively is applied to biogeography based optimization in expectation of development of BBO with better exploitation capability of the search region. The BBO with fitness difference strategy is named as fitness difference based BBO (FD-BBO). The pseudo code of proposed fitness difference based BBO (FD-BBO) approach is given in Algorithm 2.

Algorithm 2 Fitness Difference based Biogeography-Based Optimization (FD-BBO) algorithm

```
Initialize the population.
Sort the population in descending order of fitnesses.
Calculate λ and μ for each individual.
for Generation index = 1 to Maximum generation do
  According to the value of λ and μ, select an individual for migration.
  Apply migration of original BBO.
  Apply mutation of original BBO.
  if | fit^old_gbest − fit^new_gbest | ≤ fit^new_gbest × 0.01 then
    Sort the population in ascending order of fitness difference described in section 3.2.
    \\ Apply selection operator
    if fit_current x_i(Generation index) > fit_initial x_i0 then
      x_i(Generation index + 1) = x_i(Generation index)
    else
      x_i(Generation index + 1) = x_i0
    end if
  end if
  Sort the population in descending order of fitnesses.
  Apply elitism of original BBO.
  Stop, if termination criteria satisfied.
end for
```

3.5 Evaluating FD-BBO for bias(es)

It is better to obtain an idea of optimizer's intrinsic bias(es) before evaluating the performance of an optimizer using numerical experiments on benchmark set. The nature of optimizers may have central bias and/or an edge bias. Therefore, to test FD-BBO for bias(es), signature analysis [33] has been

carried out. Let us consider a minimization problem:

$$Min\ f(x,y) = 5;\ x,y \in [-5,5]$$

Clearly, every point in the search space is an optimal solution of the problem. Therefore, an unbiased optimizer should provide the solution same as random search. Signatures for BBO, BBBO (since the numerical results are compared with Blended BBO also) and FD-BBO are plotted in Figures 2(a), 2(b) and 2(c), respectively. In these signatures, solutions obtained by an algorithm in 100 runs having 1000 iterations in each run are plotted. Detailed parameter settings of these algorithms are given in section 3.6.
Let us define a solution (x, y) as an edge biased solution if

$$x \in [-5,-4] \cup [4,5] \quad \forall y \quad or$$

$$y \in [-5,-4] \cup [4,5] \quad \forall x$$

and a center biased solution if $x^2 + y^2 \leq 1$. It can be seen that the edge biased area covers 36% and center biased area covers 3.14% of the total area in the search space. These areas are shown in Figure 3.

Table 1 shows the percentage of points which lies within the considered biased areas. It is clear that BBBO is a center biased algorithm while BBO and proposed FD-BBO are almost un-biased algorithms. That is the location of the optima will have the least impact on the performance of BBO and FD-BBO.

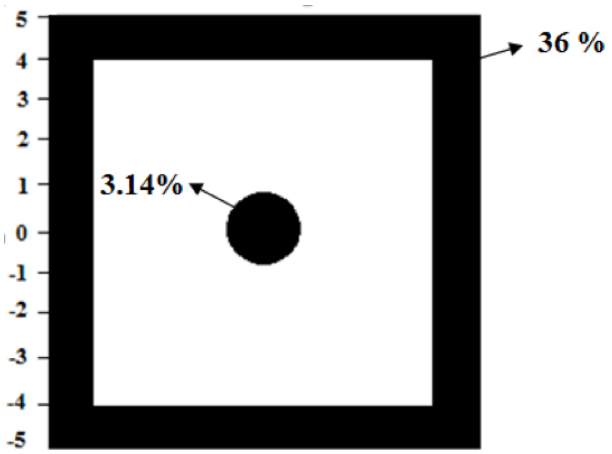

Figure 3: Edges bias and center bias areas

Table 1: Signature analysis

Biases	Percentage of points by several algorithms		
	BBO	BBBO	FD-BBO
Central bias	3.02	43.78	3.80
Edge bias	41.78	1.84	37.80

3.6 Numerical experiments, discussion and statistical analysis of FD-BBO

In this paper, we considered a set of 15 unconstrained well-known benchmark problems. These 15 benchmarks are the collection of unimodal, multimodal and hybrid composite optimization problems. For comparative study of several optimization procedures multidimensional (10 and 30- dimensional)

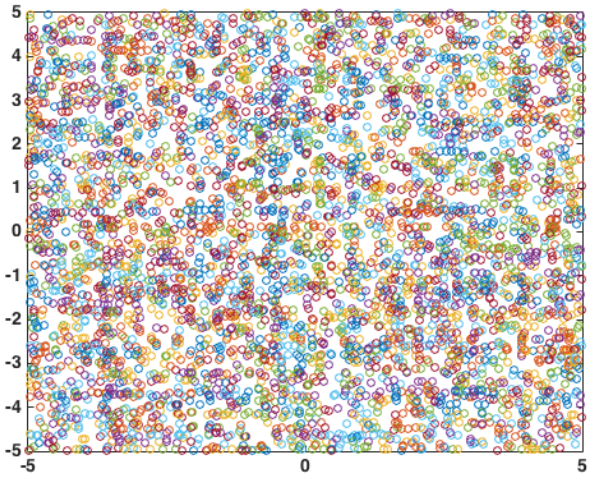

(a) Signature obtained from BBO algorithm

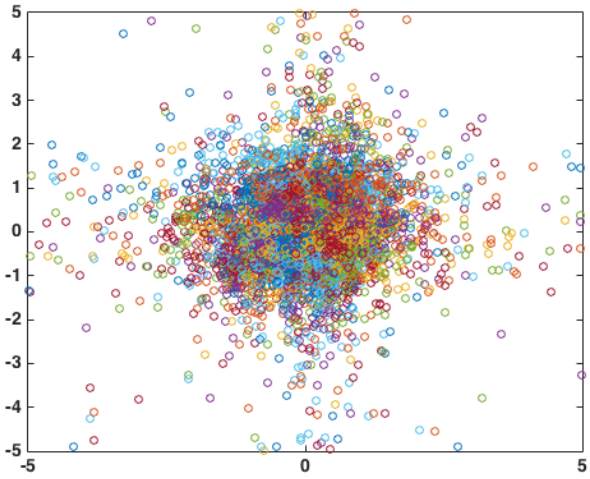

(b) Signature obtained from BBBO algorithm

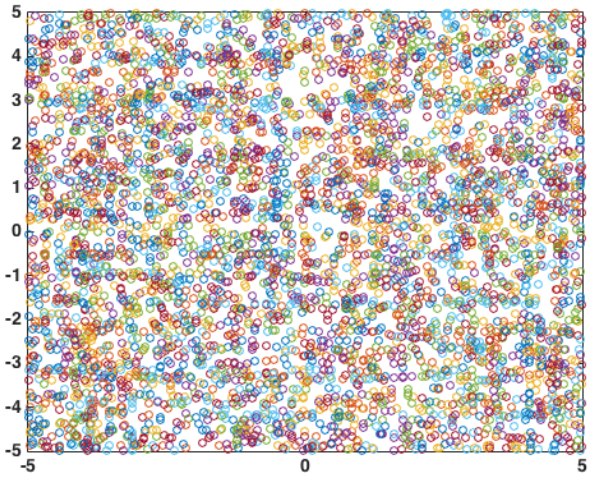

(c) Signature obtained from FD-BBO algorithm

Figure 2: Signature of algorithms

space are considered. These benchmark problems are given in Table 2 with their global optimum where f_{min} is the optimum value of function and $S \in R^D$ is search space, where R^D is Euclidean D-space (D is dimension). More details of these benchmark functions are given in Suganthan et al. [34]. In Table 2, five test problems (f_1, f_2, f_3, f_4 and f_5) are unimodal and remaining 10 test problems (f_6 - f_{15}) are multimodal. Parameters setting for the numerical experiments is as follows:
Maximum immigration rate: I = 1
Maximum emigration rate : E = 1
Mutation probability = 0.01
Elitism size = 2
Population size = 50
Maximum number of iterations = 1000
Number of runs = 100
In this work, the stopping criteria are maximum number of generation and best absolute error (E) = $\mid f(X) - f(X^*) \mid \leq \theta$, where $f(X)$ is current best value of function, $f(X^*)$ is the global optimum and θ is an acceptable error for the function. The acceptable error θ of all the considered algorithms is set to 10^{-6} for functions f_1 to f_5 and 10^{-2} for the remaining functions.
In Tables 3 and 4, we compare fitness difference based BBO (FD-BBO) with BBO and advanced version of BBO, blended BBO (BBBO). Tables 3 and 4 represent the numerical results based on basic BBO, BBBO and FD-BBO corresponding to 10 and 30-dimensional benchmark functions, respectively. Table 3 presents the minimum error ($MinE$), standard deviation (SD) and mean error (ME) of BBO, BBBO and FD-BBO for 10-dimensional problems. Table 4 presents the same for 30-dimensional problems. In Tables 3 and 4, bold entries represent the best results of the three algorithms. From these results, it is clear that FD-BBO is a better optimizer based on the minimum error ($MinE$), standard deviation (SD) and mean error (ME) for both considered dimensional (10 and 30-dimensional) space.

Table 2: Test problems [34](TP: Test problem, D: Dimension, S: Search space, f_{min} = Optimum)

TP	Objective function	S	f_{min}
f_1	Shifted sphere function	$[-100, 100]^D$	-450
f_2	Shifted Schwefels problem 1.2	$[-100, 100]^D$	-450
f_3	Shifted rotated high conditional elliptic function	$[-100, 100]^D$	-450
f_4	Shifted Schwefels problem 1.2 with noise in fitness	$[-100, 100]^D$	-450
f_5	Schwefels problem 2.6 with global optimum on bounds	$[-100, 100]^D$	-310
f_6	Shifted Rosenbrocks function	$[-100, 100]^D$	390
f_7	Shifted rotated Griewanks function without bounds	No bounds	-180
f_8	Shifted rotated Ackleys function with global optimum on bounds	$[-32, 32]^D$	-140
f_9	Shifted Rastrigins function	$[-5, 5]^D$	-330
f_{10}	Shifted rotated Rastrigins function	$[-5, 5]^D$	-330
f_{11}	Shifted rotated Weierstrass function	$[-0.5, 0.5]^D$	90
f_{12}	Schwefels problem 2.13	$[\pi, \pi]^D$	-460
f_{13}	Expanded extended Griewanks plus Rosenbrocks function	$[-3, 1]^D$	-130
f_{14}	Shifted rotated expanded Scaffers	$[-100, 100]^D$	-300
f_{15}	Hybrid composite function	$[-5, 5]^D$	120

Table 3: Comparison of results of BBO, BBBO and FD-BBO for 10-dimensional problems (TP: Test problem, Min E = Minimum error, SD = Standard deviation, ME = Mean error)

TP	Algorithm	Min E	SD	ME
f_1	BBO	2.4617E-02	6.4588E-02	1.0041E-01
	BBBO	**7.6819E-04**	2.5012E-02	**2.6778E-02**
	FD-BBO	4.0935E-03	**2.2137E-02**	2.8049E-02
f_2	BBO	1.4006E+01	1.1067E+02	1.1199E+02
	BBBO	2.6916E+01	1.1713E+02	1.8285E+02
	FD-BBO	**5.8954E-01**	**2.6870E+00**	**6.3194E+00**
f_3	BBO	9.8673E+05	4.9524E+06	7.7719E+06
	BBBO	1.0348E+06	3.4284E+06	6.0936E+06
	FD-BBO	**2.7731E+04**	**1.7557E+05**	**3.0033E+05**
f_4	BBO	4.7471E+01	5.9329E+02	5.2255E+02

	BBBO	7.0507E+02	1.5748E+03	2.7125E+03
	FD-BBO	**9.1345E-01**	**7.1893E+01**	**9.1644E+01**
f_5	BBO	5.9503E+01	8.5931E+02	8.7892E+02
	BBBO	1.2415E+03	1.4186E+03	3.4340E+03
	FD-BBO	**8.5954E+00**	**4.6115E+02**	**3.8738E+02**
f_6	BBO	1.2517E+01	2.2913E+02	2.1786E+02
	BBBO	7.3792E+00	2.3380E+02	1.9822E+02
	FD-BBO	**1.8530E-01**	**1.5012E+02**	**9.5420E+01**
f_7	BBO	3.7687E+02	2.1641E+02	8.6715E+02
	BBBO	3.7628E+02	2.4282E+02	8.9723E+02
	FD-BBO	**8.6161E+01**	**2.0974E+02**	**7.5524E+02**
f_8	BBO	2.0141E+01	7.2909E-02	2.0910E+01
	BBBO	2.0200E+01	**6.9727E-02**	2.0792E+01
	FD-BBO	**2.1633E+00**	7.2796E-02	**2.0003E+01**
f_9	BBO	8.9149E-03	5.1345E-02	5.5177E-02
	BBBO	**3.0264E-03**	1.2956E-02	1.6702E-02
	FD-BBO	6.4574E-03	**8.8787E-03**	**3.5889E-03**
f_{10}	BBO	**4.0483E+00**	1.1921E+01	2.8729E+01
	BBBO	8.0610E+00	1.4846E+01	3.7100E+01
	FD-BBO	5.9857E+00	**1.0469E+01**	**2.0794E+01**
f_{11}	BBO	2.0851E+00	5.9410E-01	3.2491E+00
	BBBO	1.8590E+00	5.6747E-01	3.1773E+00
	FD-BBO	**9.4410E-02**	**4.4792E-01**	**2.0012E+00**
f_{12}	BBO	2.5632E+04	4.9307E+04	9.0889E+04
	BBBO	1.2272E+05	1.0961E+05	3.1746E+05
	FD-BBO	**1.5690E+04**	**4.3856E+04**	**8.6478E+04**
f_{13}	BBO	2.7865E-02	**1.4534E-01**	2.1992E-01
	BBBO	1.2529E-01	2.8279E-01	4.6183E-01
	FD-BBO	**4.8146E-03**	1.6039E-01	**2.1897E-01**
f_{14}	BBO	3.2650E+00	**2.5751E-01**	3.8253E+00
	BBBO	2.9269E+00	3.0891E-01	3.7427E+00
	FD-BBO	**8.4217E-01**	3.3399E-01	**3.5728E+00**
f_{15}	BBO	1.5435E-01	**2.1332E+02**	3.8426E+02
	BBBO	**3.1769E-02**	2.4464E+02	3.7389E+02
	FD-BBO	4.6201E-02	2.1548E+02	**9.1573E+01**

Table 4: Comparison of results of BBO, BBBO and FD-BBO for 30-dimensional problems(TP: Test problem, Min E = Minimum error, SD = Standard deviation, ME = Mean error)

TP	Algorithm	Min E	SD	ME
f_1	BBO	**1.6573E+00**	1.5831E+00	4.1947E+00
	BBBO	1.8028E+01	1.8912E+01	4.1695E+01
	FD-BBO	3.9282E-01	**4.2761E-01**	**1.2902E+00**
f_2	BBO	3.3139E+03	4.2894E+03	1.1059E+04
	BBBO	3.9740E+03	1.6836E+03	6.7517E+03
	FD-BBO	**2.9032E+03**	**3.6948E+02**	**9.0165E+02**
f_3	BBO	1.4449E+07	1.9453E+07	5.1113E+07
	BBBO	**9.9106E+06**	**8.6095E+06**	**2.4715E+07**
	FD-BBO	1.2960E+07	1.0847E+07	3.1411E+07
f_4	BBO	1.9067E+04	1.2022E+04	4.1006E+04
	BBBO	**1.2252E+04**	**4.7640E+03**	2.1454E+04
	FD-BBO	1.4162E+04	1.2864E+04	**2.1373E+04**
f_5	BBO	6.1906E+03	3.0269E+03	1.1402E+04
	BBBO	8.0081E+03	1.7290E+03	1.1190E+04
	FD-BBO	**1.8698E+03**	**1.5871E+03**	**1.1092E+04**

f_6	BBO	4.2721E+02	2.8497E+03	2.5133E+03
	BBBO	1.1625E+04	4.8234E+04	7.1496E+04
	FD-BBO	**9.8158E+01**	**1.9333E+03**	**9.7674E+02**
f_7	BBO	2.1197E+03	4.4551E+02	3.0821E+03
	BBBO	2.1714E+03	5.3827E+02	3.0941E+03
	FD-BBO	**1.0426E+03**	**3.0355E+02**	**3.0346E+03**
f_8	BBO	2.0934E+01	4.6289E-02	2.1030E+01
	BBBO	2.0821E+01	7.3672E-02	2.0993E+01
	FD-BBO	**8.0855E-01**	**2.0429E-02**	**2.0010E+01**
f_9	BBO	5.3783E-01	6.2624E-01	1.5123E+00
	BBBO	8.4677E+00	3.3147E+00	1.3725E+01
	FD-BBO	**3.1087E-02**	**2.0283E-01**	**5.6352E-01**
f_{10}	BBO	6.7278E+01	3.5308E+01	1.6737E+02
	BBBO	1.0885E+02	3.3999E+01	1.9952E+02
	FD-BBO	**5.0775E+00**	**2.1368E+01**	**1.1031E+02**
f_{11}	BBO	1.3131E+01	1.5468E+00	1.9974E+01
	BBBO	1.3752E+01	1.5462E+00	2.1888E+01
	FD-BBO	**1.0819E+00**	**1.1145E+00**	**1.5308E+01**
f_{12}	BBO	**9.3288E+05**	**4.2107E+05**	1.8936E+06
	BBBO	1.5834E+06	7.1076E+05	2.9137E+06
	FD-BBO	1.0290E+06	5.7236E+05	**1.8513E+06**
f_{13}	BBO	5.1194E-01	3.9303E-01	1.5398E+00
	BBBO	2.1945E+00	7.1228E-01	3.4904E+00
	FD-BBO	**6.5521E-02**	**2.2139E-02**	**1.1788E+00**
f_{14}	BBO	1.2659E+01	3.1689E-01	1.3393E+01
	BBBO	1.2196E+01	4.5169E-01	1.3411E+01
	FD-BBO	**1.4462E-01**	**3.3923E-02**	**1.2488E+00**
f_{15}	BBO	2.2802E+02	1.8146E+02	4.2334E+02
	BBBO	5.6373E+01	1.6156E+02	4.3050E+02
	FD-BBO	**6.5492E-01**	**9.4871E+01**	**2.5967E+02**

Some more intensive statistical analyses have been carried out with the numerical results of BBO, BBBO and FD-BBO. The boxplots are the empirical distribution of data. Boxplots for minimum error, standard deviation and mean error corresponding to all algorithms BBO, BBBO and FD-BBO are given in Figures 4 and 5 for 10-dimensional and 30-dimensional problems, respectively. From the boxplot analyses, FD-BBO performs better than other considered algorithms for 10 and 30-dimensional problems. To see the significant difference between two algorithms among considered algorithms a non-parametric test, Mann-Whitney U rank sum test is applied. The results of Mann-Whitney U rank sum test for minimum error of 100 simulations are given in Table 5. In Table 5, '+' sign appears if FD-BBO is the better algorithm, '-' sign appears if FD-BBO is the worse algorithm and '=' sign appears if FD-BBO is not significantly different than compared algorithms. There are 24 '+' signs out of 30 comparisons and 22 '+' signs out of 30 comparisons in Table 5 for 10 and 30-dimensional problems, respectively. Therefore, the conclusion from all analyses is that FD-BBO is significantly a better optimizer than BBO and BBBO.

4 Wind farm layout problem formulation

4.1 Wind farm model

There are some assumptions in wind farm modeling. The wake model in this study is considered from N. O. Jenson model [5, 35]. In this wake model momentum is conserved. The downstream wind speed in j^{th} turbine under the influence of i^{th} turbine is calculated by

$$u_j = u_{0j}\left[1 - \frac{2a}{(1+\alpha_i \frac{d_{ij}}{r_i'})^2}\right] \tag{9}$$

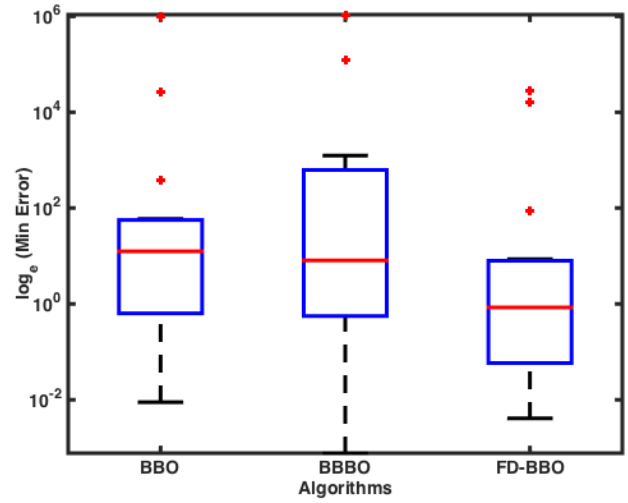

(a)

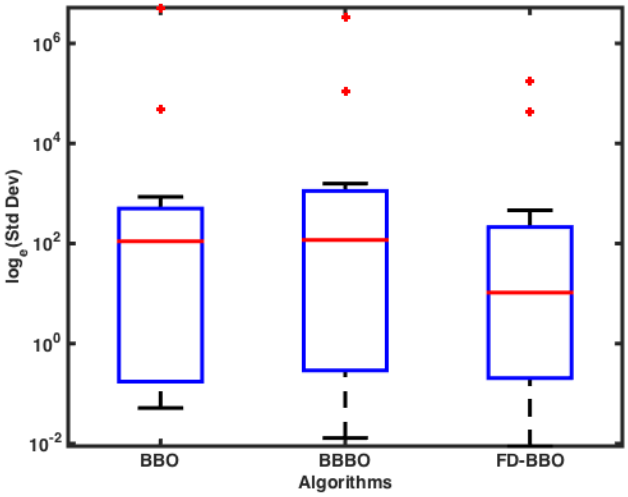

(b)

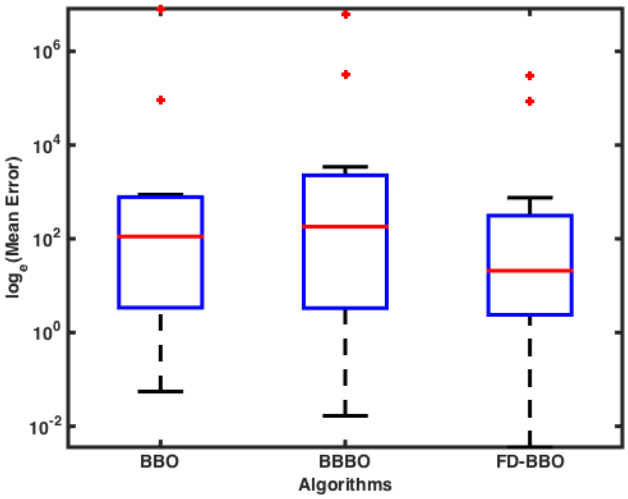

(c)

Figure 4: Boxplots for 10 Dimensional problems

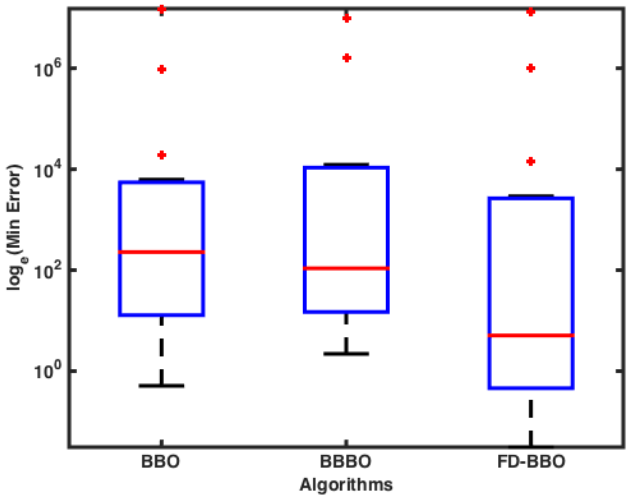

(a)

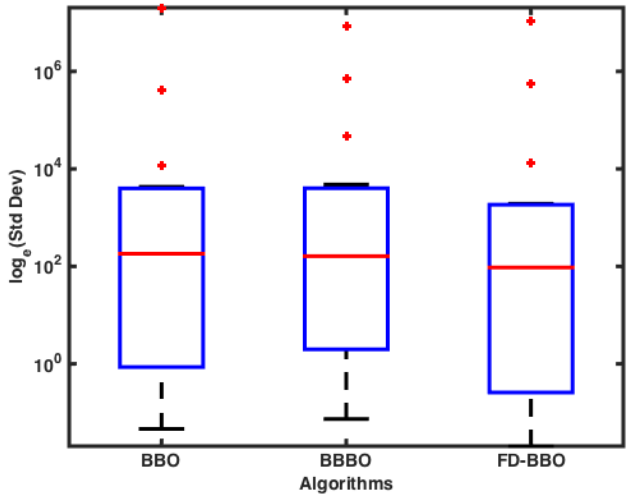

(b)

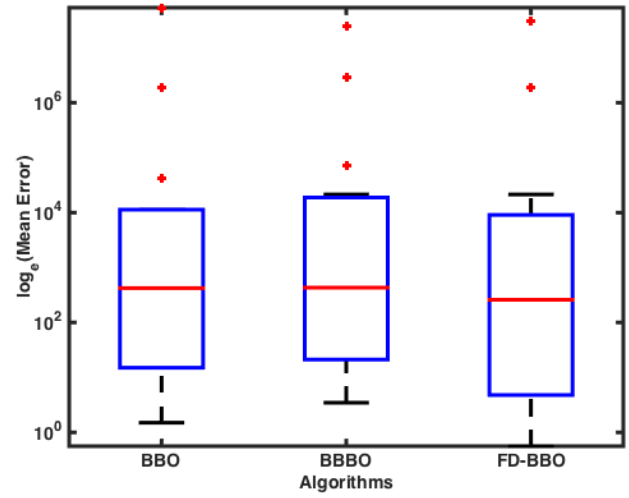

(c)

Figure 5: Boxplots for 30 Dimensional problems

Table 5: Mann-Whitney U rank sum test (TP: Test Problem)

For 10-dimensional problems			For-30 dimensional problems		
TP	FD-BBO Vs BBO	FD-BBO Vs BBBO	TP	FD-BBO Vs BBO	FD-BBO Vs BBBO
f_1	=	=	f_1	=	+
f_2	+	+	f_2	+	+
f_3	+	+	f_3	+	-
f_4	+	+	f_4	+	+
f_5	+	+	f_5	+	+
f_6	+	=	f_6	+	+
f_7	+	+	f_7	+	+
f_8	+	+	f_8	=	=
f_9	+	+	f_9	+	+
f_{10}	+	+	f_{10}	+	+
f_{11}	+	+	f_{11}	+	+
f_{12}	+	+	f_{12}	+	+
f_{13}	=	+	f_{13}	=	=
f_{14}	=	=	f_{14}	=	=
f_{15}	+	+	f_{15}	+	+
Total number of '+' signs	12	12	Total number of '+' signs	11	11

$$a = \frac{1 - \sqrt{(1 - C_T)}}{2} \tag{10}$$

$$r_i' = r_i \sqrt{\left(\frac{1-a}{1-2a}\right)} \tag{11}$$

$$\alpha_i = \frac{0.5}{ln(\frac{h_i}{z_0})} \tag{12}$$

Where, u_{0j} is the free stream wind speed at j^{th} turbine
a is the axial induction factor
d_{ij} is the distance between i^{th} and j^{th} turbine
r_i is the rotor radius of i^{th} turbine
r_i' is the downstream rotor radius of i^{th} turbine
h_i is the hub height of i^{th} turbine
C_T is the thrust coefficient of the wind turbine, which is considered same for all turbines
α_i is the entrainment constant pertaining to i^{th} turbine
z_0 is the surface roughness of wind farm
The wake region is conical for the linear wake model and radius of the wake region is represented by wake influence radius which is defined as:

$$R_{wi} = \alpha_i d_{ij} + r_i' \tag{13}$$

A linear wake model of j^{th} turbine under the influence of i^{th} turbine is shown in Figure 6.
At an instant any wind turbine is under the multiple wake region, i.e. wind turbines' velocity is influenced by multiple wakes. The wind speed of i^{th} turbine is calculated using the assumption that kinetic energy deficit of the mixed wake is equal to the sum of the energy deficits as follows:

$$u_k = u_{0k}\left[1 - \sqrt{\sum_{m=1}^{N_T}\left(1 - \frac{u_{km}}{u_{0m}}\right)^2}\right] \tag{14}$$

Where u_{0k} and u_{0m} are free stream wind velocity without wake effect at k^{th} and m^{th} turbine, respectively. u_{km} is the wind velocity at k^{th} turbine under the wake region of m^{th} turbine. N_T is the total number of turbines influencing the k^{th} turbine with wake effect.
Here we have considered a constant wind speed and fixed wind direction (south to north). Total power output for each turbine in one year is calculated as:

$$P_i = 0.5 * \rho * \pi * r_i^2 * u_i^3 * \frac{C_p}{1000} \quad kW, \quad i = 1, 2, ..., N_T \tag{15}$$

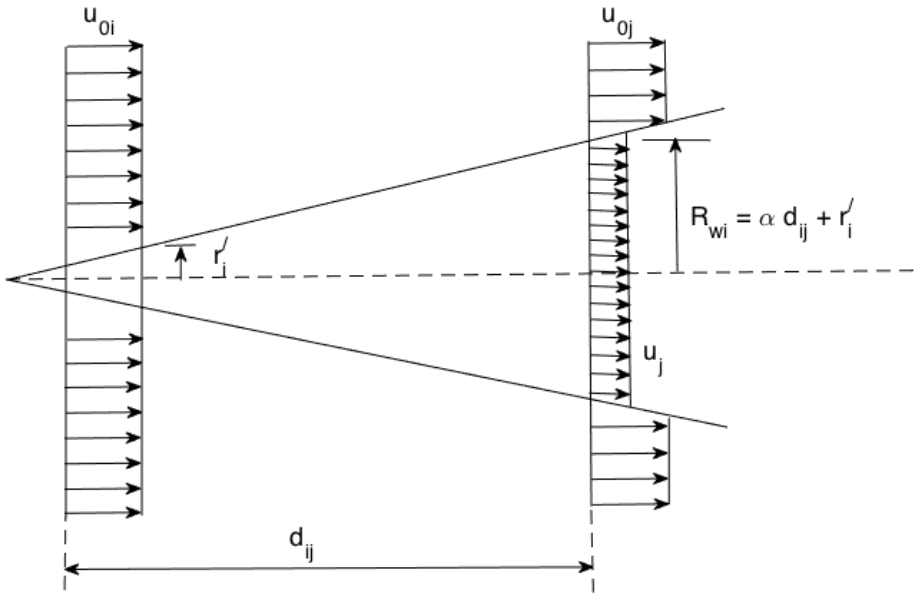

Figure 6: Linear wake model of wind turbine

Where ρ represents the air density and C_p represents the rotor efficiency.
The total power generated by wind farm in one year is calculated as:

$$P_{total} = \sum_{i=1}^{N_T} P_i \tag{16}$$

We considered Mosetti's cost model having N_T number of turbines as:

$$Cost = N_T\left(\frac{2}{3} + \frac{1}{3}\exp^{-0.00174N_T^2}\right) \tag{17}$$

In this study, turbines' position are intersection points of the grid within the wind farm. We are not considering the boundary of the wind farm as the potential location for turbines.
The main objective of the study is highest power output at minimum cost and can be formulated as:

$$Objective = \frac{Cost}{P_{total}} \tag{18}$$

4.2 FD-BBO for wind farm layout optimization problem

In the literature, many non-conventional techniques, e.g. genetic algorithm (GA), Monte Carlo simulation, Greedy algorithm, BBO, Cuckoo search etc. have been applied to solve wind farm layout optimization problem. In the earlier studies, researchers have tried to find the optimal placement of wind turbines so that power generation of wind farm maximizes. Now a days researchers are dealing to find out the optimal configuration of wind turbines such as hub height and rotor radius along with the optimal location of wind turbines. The results are motivating as compared to earlier studies. Therefore, fitness difference based BBO approach is explored to find wind farm layout with optimal configurations (hub heights and rotor radii) of wind turbines.
We considered a square wind farm of size $2000m \times 2000m$. The wind farm is subdivided into 100 grids each of size $200m \times 200m$. If we consider N_T number of turbines whose hub heights and rotor radii are not necessarily to be uniform to be placed, then any arrangement of these N_T turbines in a two-dimensional wind farm with several hub heights and rotor radii represent a potential solution in FD-BBO. Thus i^{th} solution is represented by $(x_i^t,\ y_i^t,\ h_i^t,\ r_i^t)$. Where $(x_i^t,\ y_i^t)$ is the position of t^{th}

turbine while h_i^t and r_i^t are the hub height and rotor radius of t^{th} turbine, respectively. Clearly, the number of decision variables in this problem are $4N_T$. The step by step procedure to solve wind farm layout and configuration problem by FD-BBO is given in Algorithm 3.

Algorithm 3 FD-BBO for wind farm layout optimization

Initialize the solution (habitat) (x_i^t, y_i^t, h_i^t, r_i^t), t = 1, 2, ...,N_T; i = 1, 2, ..., N_p.
Compute u_t, P_t and P_{total} using equations 14, 15 and 16.
Calculate λ and μ using equations 4 and 5.
Sort the population to decreasing order of total power output (P_{total}) of the wind farm.
for *Generation index* = 1 to *Maximum generation* **do**
  According to the value of λ and μ, select habitat for migration.
  Apply migration as in Algorithm 1.
  Apply mutation as in Algorithm 1.
  if $\mid {P_{total}}_{gbest}^{old} - {P_{total}}_{gbest}^{new} \mid \leq {P_{total}}_{gbest}^{new} \times 0.01$ **then**
    Apply fitness difference based sorting strategy described in section 3.2.
  end if
  Compute u_t, P_t and P_{total} for updated solutions.
  Sort the population to decreasing order of total power output (P_{total}) of the wind farm.
  Keep the elite solution.
  Stop, if termination criteria satisfied.
end for

4.3 Results and discussion

For the considered square wind farm of size $2000m \times 2000m$, air density (ρ) is 1.2254 kg/m^3, rotor efficiency (C_p) is 0.4, thrust coefficient (C_T) is 8/9 and the surface roughness of wind farm (z_0) is $0.3m$. FD-BBO, BBO and BBBO are applied to solve wind farm layout optimization problem. The parameters of these algorithms are same as in section 3.6.
In Table 6, the comparison between Mosetti et al.'s [1] results and present study results are carried out. Results are compared for 26 number of turbines. In the Mosetti et al.'s study, hub height ($h = 60m$), rotor radius ($r = 20m$) and thrust coefficient ($C_T = 0.88$) were fixed for each turbine. In the present study, we are also dealing to tune hub heights and rotor radii along with the optimal layout of wind turbines. Total power output obtained in the present study is better than that of Mosetti et al. [1] study. BBO and FD-BBO algorithms are performing better than earlier study, but FD-BBO algorithm outperforms. Table 7 presents the comparison between Grady et al. [2] results and present study's results. Results are reported for 30 number of turbines. In Grady et al. [2] study, hub height, rotor radius and thrust coefficient are same as given in Mosetti et al. [1]. In this comparison, total power output obtained by BBO and FD-BBO is better than Grady et al. approach.
Figures 7 and 8, represent the optimal configuration of wind turbines. Figure 7(a) is the optimal

Table 6: Comparison of present study results with Mosetti et al. [1] results

Parameters	Mosetti [1] study		Present study		
	Reported	Calculated (Without Approximation)	Using BBO	Using BBBO	Using FD-BBO
Number of turbine	26	26	26	26	26
Total power (kw year)	12352	12654	13653	12307	13683
Fitness value	0.0016197	0.001581	0.0014654	0.00162562	0.0014621

Table 7: Comparison of present study results with Grady et al. [2] results

Parameters	Grady [2] study		Present study		
	Reported	Calculated (Without Approximation)	Using BBO	Using BBBO	Using FD-BBO
Number of turbine	30	30	30	30	30
Total power (kw year)	14310	14667	15655	14090	15662
Fitness value	0.0015436	0.0015061	0.001411	0.00156769	0.0014103

positions of 26 wind turbines given by Mosetti et al. [1] and Figures 7(b), 7(c) and 7(d) are optimal position of 26 wind turbines by BBO, BBBO and FD-BBO algorithms, respectively. Figure 8(a) presents the optimal position of 30 wind turbine obtained by Grady's approach. Figures 8(b), 8(c) and 8(d) present the optimal position of 30 wind turbines by BBO, BBBO and FD-BBO algorithms, respectively. The corresponding hub heights and rotor radii along with position coordinates obtained by BBO, BBBO and FD-BBO approaches for 26 and 30 wind turbines are presented in Tables 8 and 9, respectively.

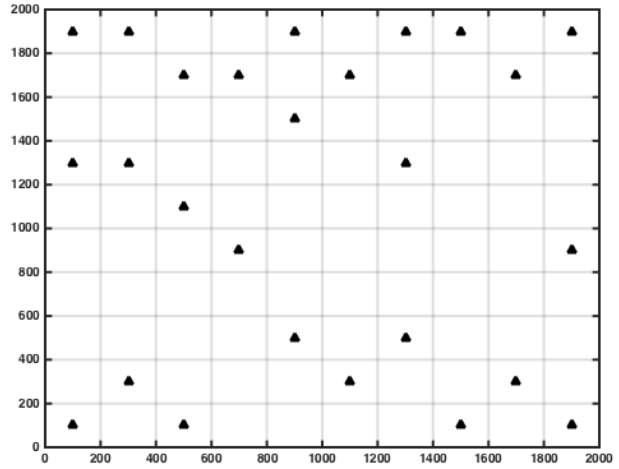

(a) By Mosetti et al. using GA

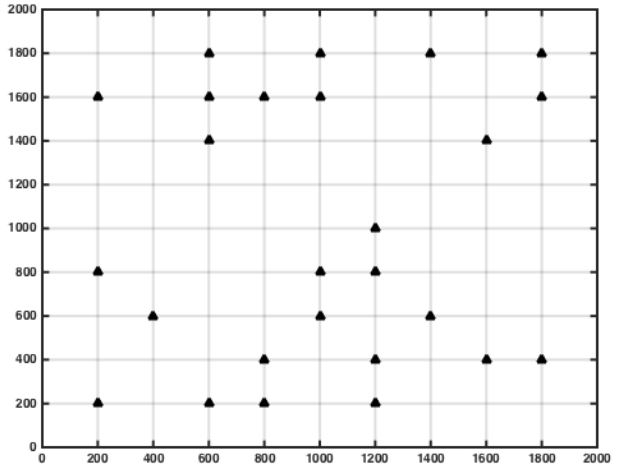

(b) By present study using BBO

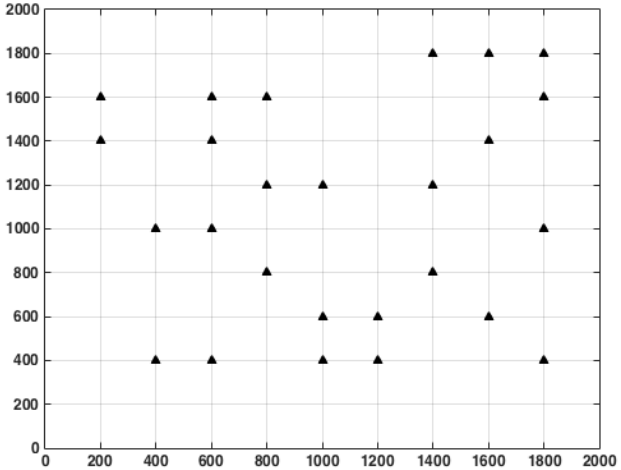

(c) By present study using BBBO

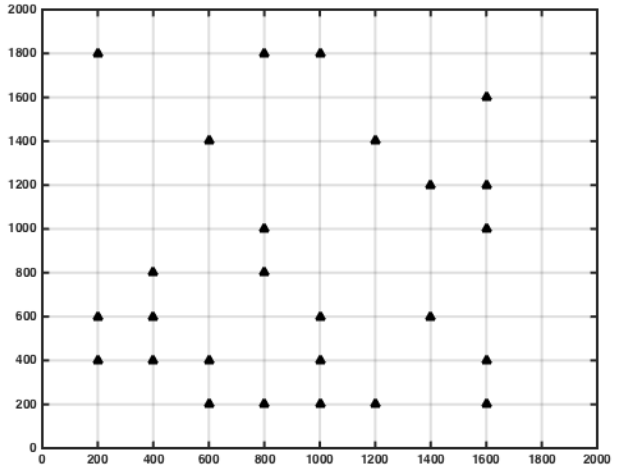

(d) By present study using FD-BBO

Figure 7: Optimal configurations of 26 wind turbines

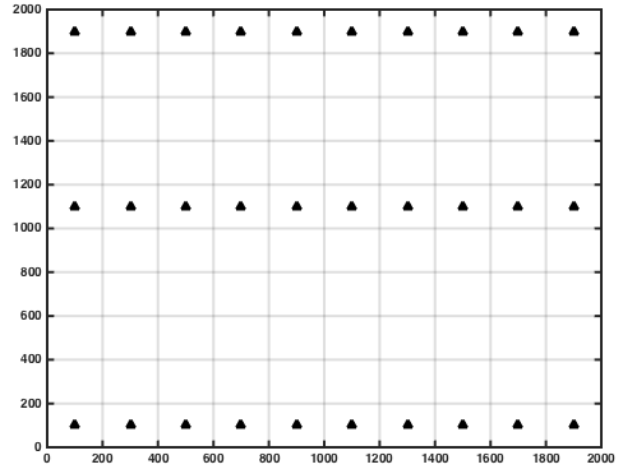

(a) By Grady et al. using GA

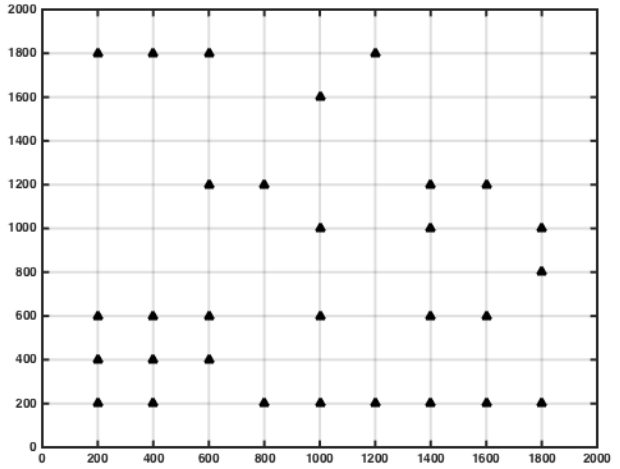

(b) By present study using BBO

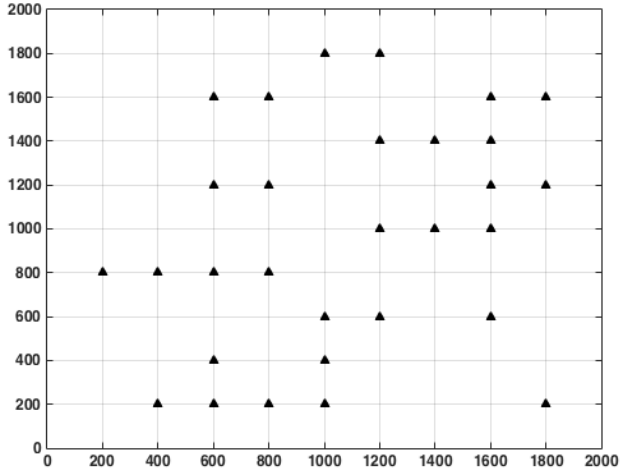

(c) By present study using BBBO

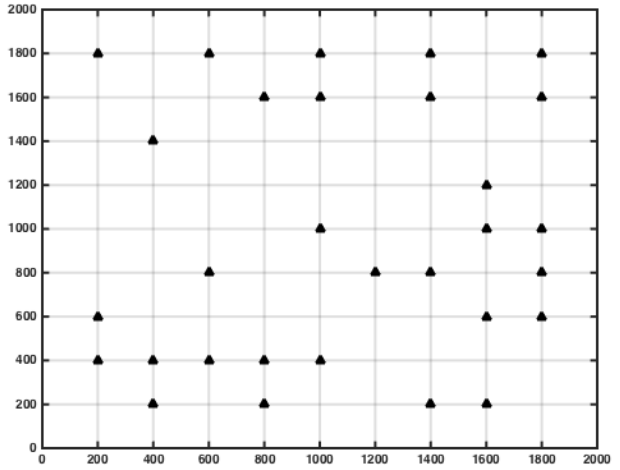

(d) By present study using FD-BBO

Figure 8: Optimal configurations of 30 wind turbines

Table 8: 26 wind turbines positions, hub heights and rotor radii obtained by BBO, BBBO and FD-BBO in a $2000m \times 2000m$ square farm

Using BBO			Using BBBO			Using FD-BBO		
Optimal position	Rotor radius	Hub height	Optimal position	Rotor radius	Hub height	Optimal position	Rotor radius	Hub height
(600, 1800)	19.9647	51.7587	(400, 1000)	19.7091	32.7375	(1600, 1600)	19.8535	44.1743
(600, 1600)	19.8356	33.3044	(1000, 1200)	18.1712	47.4873	(1200, 1400)	19.9369	31.6778
(1800, 1800)	19.9471	25.3969	(1600, 1800)	19.5334	22.9533	(600, 1400)	19.9466	46.6166
(200, 1600)	19.7876	42.0720	(600, 1600)	17.2568	30.6825	(1400, 1200)	19.9668	37.3379
(600, 1400)	19.9381	34.0635	(200, 1600)	18.5133	22.6059	(1600, 1200)	19.9485	42.4154
(1000, 1800)	19.8236	43.1484	(600, 1400)	18.1056	28.4428	(400, 800)	19.7576	33.8037
(1000, 1600)	19.9443	41.0037	(600, 1000)	17.3077	25.8279	(1600, 1000)	19.9701	48.2209
(1400, 1800)	19.6782	20.5167	(400, 400)	18.9681	32.3002	(600, 400)	19.7962	34.7141
(1000, 800)	19.8934	47.2696	(800, 1600)	18.5899	54.1832	(200, 1800)	19.8521	46.0036
(800, 1600)	19.5185	53.0970	(600, 400)	19.6350	51.2949	(400, 600)	19.9661	35.3177
(800, 400)	19.9536	39.7455	(1400, 1800)	18.6810	49.9452	(200, 600)	19.9169	40.1456
(1200, 1000)	19.9330	32.9198	(1800, 1800)	19.6675	40.5307	(1600, 400)	19.9015	52.7761
(200, 800)	19.9656	27.6139	(1800, 1600)	18.6534	53.9258	(1000, 1800)	19.9519	36.4000
(800, 200)	19.8181	21.2555	(1000, 600)	18.7560	55.5234	(1000, 600)	19.6389	21.6649
(1800, 1600)	19.8929	42.6978	(1400, 1200)	19.9923	59.7716	(1400, 600)	19.8843	31.7090
(1000, 600)	19.9764	32.9999	(1200, 600)	19.5760	22.8167	(800, 1800)	19.6078	21.0827
(1600, 1400)	19.8703	31.6229	(1200, 400)	18.9420	44.3078	(800, 1000)	19.8852	43.0994
(1800, 400)	19.9220	57.2311	(1800, 1000)	18.4184	20.3368	(400, 400)	19.9487	37.7021
(400, 600)	19.9988	51.5441	(1400, 800)	18.1485	40.9401	(800, 800)	19.7267	47.7567
(1200, 800)	19.9734	23.4229	(200, 1400)	19.5030	33.3717	(1000, 400)	19.9772	59.8607
(600, 200)	19.6576	47.3918	(800, 1200)	19.5509	42.7233	(600, 200)	19.9696	43.4479
(1400, 600)	19.6436	26.6658	(1600, 1400)	17.9891	29.9358	(200, 400)	19.9387	38.6388
(1200, 400)	19.9544	57.3936	(1000, 400)	18.9600	49.8480	(1200, 200)	19.9450	55.3500
(1200, 200)	19.7656	43.7386	(1600, 600)	19.8247	51.0533	(800, 200)	19.9233	44.1171
(1600, 400)	19.8683	30.2834	(1800, 400)	19.4638	35.5381	(1600, 200)	19.9372	44.2013
(200, 200)	19.9936	56.3159	(800, 800)	18.1130	37.9484	(1000, 200)	19.9414	28.0759

Table 9: 30 wind turbines positions, hub heights and rotor radii obtained by BBO, BBBO and FD-BBO in a $2000m \times 2000m$ square farm

Using BBO			Using BBBO			Using FD-BBO		
Optimal position	Rotor radius	Hub height	Optimal position	Rotor radius	Hub height	Optimal position	Rotor radius	Hub height
(600, 1800)	19.9794	49.2502	(1000, 1800)	18.4216	44.5251	(600, 1800)	19.4316	29.4083
(200, 1800)	19.9533	47.0476	(800, 1600)	18.8931	37.8571	(1800, 1800)	19.9252	49.6617
(1200, 1800)	19.9521	27.8465	(1400, 1400)	18.8165	57.4066	(600, 800)	19.9679	50.2845
(400, 1800)	19.9832	37.4665	(1200, 1800)	17.3464	53.0912	(800, 1600)	19.9843	29.9192
(1000, 1600)	19.7984	56.7558	(600, 1600)	18.9351	22.4174	(1800, 1600)	19.8893	53.4238
(1800, 1000)	19.8607	58.2722	(800, 1200)	19.5773	55.1218	(600, 400)	19.7590	39.1783
(1600, 1200)	19.8335	50.4844	(800, 800)	19.1297	51.5130	(1400, 1800)	19.9329	25.1884
(200, 600)	19.1115	58.6931	(600, 1200)	18.8977	38.6689	(1000, 1800)	19.9310	49.7733
(1000, 1000)	19.9443	38.8130	(600, 800)	19.2367	51.7145	(800, 400)	19.9947	57.7767
(1600, 600)	19.8536	58.1634	(200, 800)	19.5784	42.4235	(400, 1400)	19.8710	30.3715
(600, 1200)	19.5502	50.7616	(1200, 1400)	19.1018	50.5052	(1400, 1600)	19.8973	32.8607
(600, 600)	19.7520	33.4019	(1000, 600)	19.8819	29.5753	(400, 400)	19.6900	39.9654
(1800, 800)	19.8077	26.6128	(600, 400)	18.9865	54.3138	(200, 1800)	19.6931	50.0896
(1400, 1200)	19.7821	42.7594	(1000, 400)	19.4693	43.5557	(1800, 1000)	19.8026	55.7636
(600, 400)	19.9456	24.4669	(800, 200)	18.6991	55.7785	(200, 600)	19.7797	51.3783
(400, 600)	19.6468	42.4717	(1600, 1600)	19.8078	58.1218	(200, 400)	19.7526	45.5725
(1400, 1000)	19.9953	28.4426	(400, 800)	18.8033	28.4088	(1000, 1600)	19.9535	58.7362
(1600, 200)	19.7998	26.6100	(600, 200)	19.7916	33.5676	(400, 200)	19.6580	33.8476
(200, 400)	19.9044	33.4797	(1000, 200)	18.8068	20.9897	(1200, 800)	19.6410	47.6596
(1000, 600)	19.7792	47.2829	(1400, 1000)	17.1594	29.2716	(1400, 800)	19.9477	55.6132
(200, 200)	19.9654	45.4332	(1800, 1600)	17.8168	36.6510	(800, 200)	19.8440	26.8447
(1200, 200)	19.7980	58.8234	(1200, 1000)	19.5788	53.3900	(1600, 1200)	19.9954	54.4604
(1000, 200)	19.8976	35.8667	(1200, 600)	14.5978	34.3058	(1600, 1000)	19.7439	53.0715
(1400, 600)	19.9817	22.5718	(1600, 1400)	19.7690	39.1186	(1400, 200)	19.9998	22.5858
(800, 1200)	19.7910	36.9339	(1600, 1200)	17.7152	51.7474	(1600, 600)	19.9601	44.5301
(400, 400)	19.9749	34.4737	(1600, 1000)	18.3185	55.6551	(1000, 1000)	19.6361	47.8160
(1800, 200)	19.8868	47.4931	(1800, 1200)	19.5529	56.4666	(1800, 800)	19.2492	20.1137
(400, 200)	19.3745	19.8123	(1800, 200)	17.6082	25.6741	(1600, 200)	19.8545	46.0326
(1400, 200)	19.9383	56.3447	(400, 200)	18.6487	48.2097	(1000, 400)	19.7053	53.1190
(800, 200)	19.2541	28.0815	(1600, 600)	19.7819	58.0076	(1800, 600)	19.7639	39.1860

From the observation of results reported in Tables 8 and 9, there are variations of hub heights and rotor radii in wind turbines. Practically, many variants of rotor radii and hub heights as the number of turbines are not possible. For practical purpose three different rotor radii and hub heights are selected for both the cases from Tables 8 and 9. For 26 wind turbines three rotor radii ($R_1 = 19.8934$, $R_2 = 18.9420$ and $R_3 = 19.9369$) and three hub heights ($H_1 = 39.7455$, $H_2 = 40.5307$ and $H_3 = 42.4154$) are selected from Table 8. These selected rotor radii R_1, R_2 and R_3 are the median of columns 2, 5 and 8, respectively. Observed hub heights H_1, H_2 and H_3 are the median of columns 3, 6 and 9, respectively. In case of 30-wind turbines, three rotor radii and three hub heights are selected from Table 9 through the same observation. Here three different rotor radii ($R'_1 = 19.8571$, $R'_2 = 18.9164$ and $R'_3 = 19.8492$) and three different hub heights ($H'_1 = 40.6423$, $H'_2 = 46.3674$ and $H'_3 = 46.8461$) are observed. Considered rotor radii R'_1, R'_2 and R'_3 are the median of columns 2, 5 and 8, respectively as well as three hub heights H'_1, H'_2 and H'_3 are the median of columns 3, 6 and 9, respectively.
Again optimal position of wind turbines are reproduced from observed set of rotor radii and hub heights for both cases. The increased total power output of wind farm for both the cases are reported in Tables 10 and 11. Thus the optimal layout corresponding to given Tables 10 and 11 are represented in Figures 9 and 10, respectively. In Figure 9, we can see the final optimal configuration of 26-wind turbines achieved by three techniques. Figures 9(a), 9(b) and 9(c) represent the optimal layout of wind turbines using BBO, BBBO and FD-BBO, respectively. In Figure 9(a) and 9(b), all 26-wind turbines have different three choices of rotor radii (R_1, R_2, R_3) as well as hub heights (H_1, H_2, H_3). But in Figure 9(c), all wind turbines have unique rotor radius (R_3) along with the variation of hub heights (H_1, H_2, H_3). Similarly, in Figure 10, the final optimal configuration of 30-wind turbines are given which is again achieved by three techniques. Figures 10(a), 10(b) and 10(c), represent the optimal layout of wind turbines using BBO, BBBO and FD-BBO, respectively. Here in Figures 10(a) and 10(b), all 30-wind turbines have different choices of rotor radii (R'_1, R'_2, R'_3) as well as hub heights (H'_1, H'_2, H'_3). In Figure 10(c), corresponding to several hub heights (H'_1, H'_2, H'_3) there is one rotor radius (R'_1) is obtained by FD-BBO. Therefore, FD-BBO is considered a good optimizer to find the optimal rotor radii (R_3) and (R'_1) corresponding to the cases 26-wind turbines and 30-wind turbines, respectively.
The corresponding position co-ordinates of 26-wind turbines along with hub heights and rotor radii using considered algorithms are given in Table 12. In case of 26-wind turbines, it is observed from the above discussion that FD-BBO gives the promising solution by selecting best rotor radius ($R_3 = 19.9369$) from the given rotor radii (R_1, R_2 and R_3). The recommended rotor radius R_3 is the median of rotor radii obtained by FD-BBO. The obtained energy production reported in Tables 10 shows that FD-BBO outperforms over BBO and BBBO. Again the same analysis is done for 30-wind turbines. Here in Table 13, the corresponding position co-ordinates along with hub heights and rotor radii using considered algorithms are given. Again FD-BBO outperforms over BBO and BBBO by selecting the best rotor radius ($R'_1 = 19.8571$) among the given set of rotor radii (R'_1, R'_2 and R'_3).
Through these analysis of the results for both the cases (26-wind turbines and 30-wind turbines) given in Tables 10, 11, 12 and 13, FD-BBO is recommended a good optimizer to find the optimal configuration of wind turbines. In both the cases, FD-BBO recommends the best rotor radius from the given set of rotor radii. Also FD-BBO is able to find the best optimal placement of wind turbines along with suitable hub heights. The above discussion clearly shows the performance of FD-BBO is better than BBO and blended BBO. FD-BBO is able to find the best rotor radius which is most convenient and reliable to constructing the promising wind farm. Therefore, FD-BBO is better optimizer for selecting most appropriate rotor radius along with suitable hub height to produce the maximum energy.

Table 10: Final energy output of wind farm for case 1

Parameter	Using BBO	Using BBBO	Using FD-BBO
Number of turbine	26	26	26
Total power (kw year)	13745	13620	13750
Fitness value	0.00145550	0.00146888	0.00145510

Table 11: Final energy output of wind farm for case 2

Parameter	Using BBO	Using BBBO	Using FD-BBO
Number of turbine	30	30	30
Total power (kw year)	15736	15460	15738
Fitness value	0.00140374	0.00142874	0.00140352

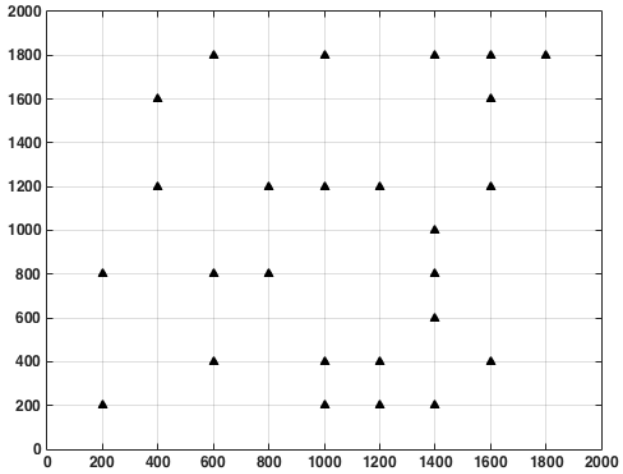

(a) Final layout using BBO

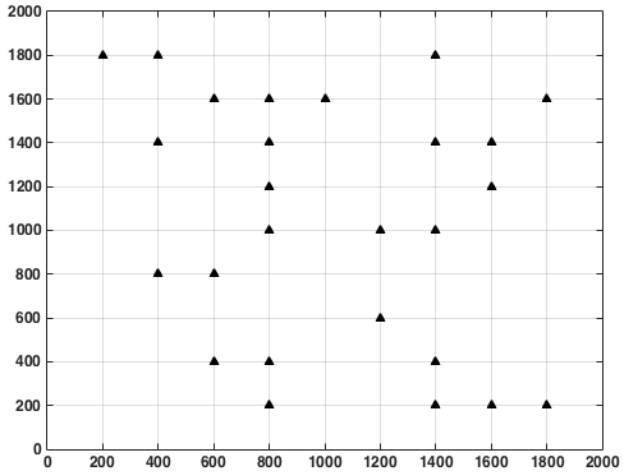

(b) Final layout using BBBO

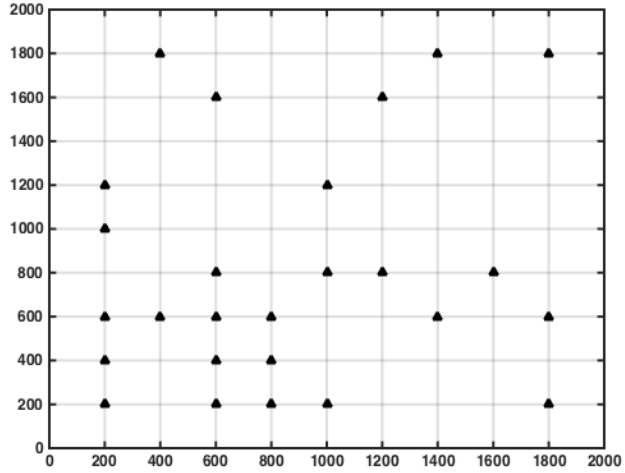

(c) Final layout using FD-BBO

Figure 9: Final optimal configurations of 26 wind turbines

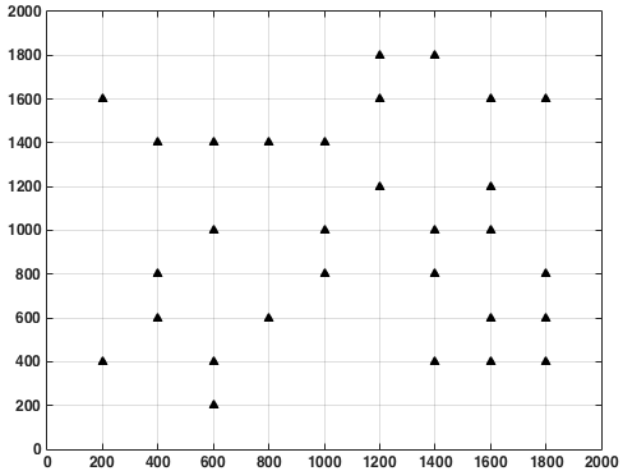

(a) Final layout using BBO

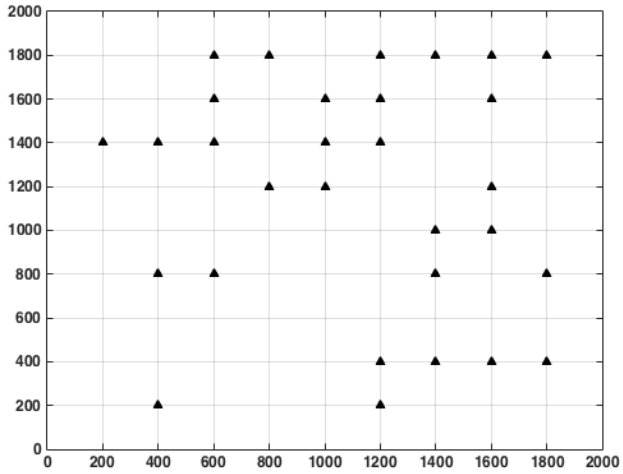

(b) Final layout using BBBO

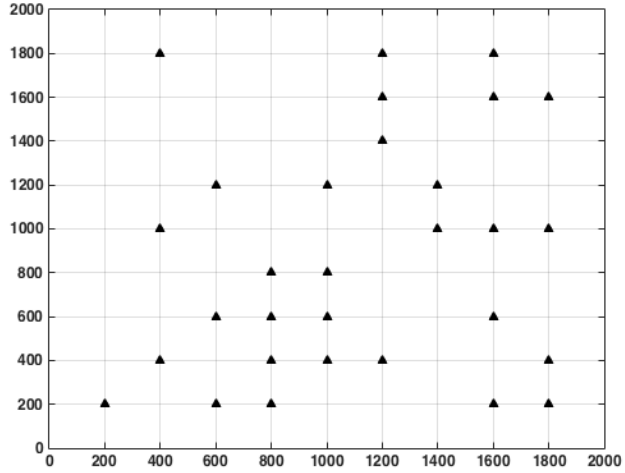

(c) Final layout using FD-BBO

Figure 10: Final optimal configurations of 30 wind turbines

Table 12: Final 26 wind turbines positions, hub heights and rotor radii obtained by BBO, BBBO and FD-BBO in a $2000m \times 2000m$ square farm

Using BBO			Using BBBO			Using FD-BBO		
Optimal position	Rotor radius	Hub height	Optimal position	Rotor radius	Hub height	Optimal position	Rotor radius	Hub height
(1000, 1800)	19.9369	40.5307	(1400, 1800)	19.9369	40.5307	(400, 1800)	19.9369	42.4154
(1400, 1800)	19.9369	39.7455	(600, 1600)	19.9369	40.5307	(600, 1600)	19.9369	40.5307
(1200, 1200)	19.8934	42.4154	(1400, 1400)	19.9369	40.5307	(600, 800)	19.9369	42.4154
(1400, 1000)	19.9369	40.5307	(800, 1400)	19.8934	42.4154	(1000, 1200)	19.9369	40.5307
(1200, 400)	19.9369	42.4154	(600, 800)	19.8934	40.5307	(1200, 1600)	19.9369	40.5307
(800, 1200)	19.9369	42.4154	(800, 1200)	19.9369	40.5307	(600, 600)	19.9369	40.5307
(400, 1600)	19.9369	42.4154	(1400, 1000)	19.8934	42.4154	(1000, 800)	19.9369	40.5307
(1800, 1800)	19.9369	42.4154	(600, 400)	19.8934	42.4154	(1800, 1800)	19.9369	39.7455
(600, 1800)	19.9369	40.5307	(1400, 400)	19.9369	40.5307	(1200, 800)	19.9369	42.4154
(1600, 1800)	19.9369	42.4154	(800, 1000)	19.8934	40.5307	(1800, 600)	19.9369	40.5307
(600, 800)	19.9369	39.7455	(1200, 1000)	19.9369	39.7455	(600, 400)	19.9369	42.4154
(1000, 1200)	19.8934	42.4154	(400, 1800)	19.9369	42.4154	(800, 600)	19.9369	40.5307
(1000, 400)	19.9369	40.5307	(1600, 1400)	19.8934	40.5307	(1800, 200)	19.9369	40.5307
(800, 800)	19.9369	42.4154	(400, 1400)	19.9369	40.5307	(1400, 1800)	19.9369	40.5307
(1400, 800)	19.9369	40.5307	(1800, 200)	19.9369	39.7455	(400, 600)	19.9369	40.5307
(200, 800)	19.9369	39.7455	(800, 400)	19.9369	39.7455	(600, 200)	19.9369	40.5307
(600, 400)	19.9369	40.5307	(1400, 200)	19.9369	40.5307	(1600, 800)	19.9369	40.5307
(1200, 200)	19.9369	42.4154	(1800, 1600)	19.9369	42.4154	(200, 1200)	19.9369	40.5307
(400, 1200)	19.9369	42.4154	(400, 800)	19.9369	42.4154	(200, 1000)	19.9369	39.7455
(200, 200)	19.9369	42.4154	(200, 1800)	19.9369	40.5307	(800, 400)	19.9369	40.5307
(1400, 600)	19.9369	42.4154	(1600, 1200)	19.9369	40.5307	(1000, 200)	19.9369	40.5307
(1600, 1600)	19.9369	40.5307	(800, 1600)	19.9369	40.5307	(200, 600)	19.9369	40.5307
(1000, 200)	19.9369	40.5307	(1600, 200)	19.9369	39.7455	(200, 400)	19.9369	40.5307
(1400, 200)	19.9369	42.4154	(1000, 1600)	19.9369	40.5307	(1400, 600)	19.9369	40.5307
(1600, 1200)	19.9369	39.7455	(800, 200)	18.942	40.5307	(200, 200)	19.9369	40.5307
(1600, 400)	19.9369	39.7455	(1200, 600)	19.9369	40.5307	(800, 200)	19.9369	42.4154

Table 13: Final 30 wind turbines positions, hub heights and rotor radii obtained by BBO, BBBO and FD-BBO in a $2000m \times 2000m$ square farm

Using BBO			Using BBBO			Using FD-BBO		
Optimal position	Rotor radius	Hub height	Optimal position	Rotor radius	Hub height	Optimal position	Rotor radius	Hub height
(1800, 1600)	19.8571	39.6423	(1800, 1800)	19.8571	39.6423	(1800, 1600)	19.8571	39.6423
(200, 1600)	19.8492	46.8961	(600, 1600)	19.8492	46.8961	(400, 1800)	19.8571	46.3674
(1000, 1400)	19.8571	39.6423	(1000, 1600)	19.8492	46.8961	(1600, 1800)	19.8571	39.6423
(1800, 800)	19.8571	46.3674	(1800, 800)	19.8571	46.3674	(600, 1200)	19.8571	46.3674
(400, 1400)	19.8492	46.3674	(400, 1400)	19.8492	46.3674	(400, 1000)	19.8571	46.3674
(1400, 1800)	19.8571	46.8961	(1400, 1800)	19.8571	46.8961	(1600, 1600)	19.8571	46.8961
(1600, 1600)	19.8571	46.3674	(1600, 1600)	19.8492	46.8961	(1400, 1200)	19.8571	46.3674
(1600, 1200)	19.8492	46.3674	(1600, 1200)	19.8492	46.3674	(1600, 1000)	19.8571	46.3674
(800, 1400)	19.8571	39.6423	(800, 1800)	19.8492	39.6423	(1000, 1200)	19.8571	39.6423
(400, 800)	19.8571	46.3674	(400, 800)	19.8571	46.3674	(1800, 1000)	19.8571	46.8961
(800, 600)	19.8571	39.6423	(800, 1200)	19.8571	39.6423	(1000, 800)	19.8571	39.6423
(200, 400)	19.8571	39.6423	(200, 1400)	19.8571	46.8961	(1800, 400)	19.8571	46.3674
(600, 1400)	19.8571	46.3674	(600, 1400)	19.8571	46.3674	(1800, 200)	19.8571	39.6423
(1000, 1000)	19.8571	46.8961	(1000, 1400)	19.8492	39.6423	(1000, 600)	19.8571	46.3674
(1000, 800)	19.8571	46.3674	(1000, 1200)	19.8571	46.3674	(800, 800)	19.8571	39.6423
(1600, 1000)	19.8571	46.3674	(1600, 1000)	19.8571	39.6423	(1600, 600)	19.8571	46.3674
(1800, 600)	19.8492	39.6423	(1800, 400)	18.9164	46.3674	(800, 600)	19.8571	46.3674
(600, 1000)	19.8571	46.3674	(600, 800)	19.8571	46.3674	(600, 600)	19.8571	46.3674
(1600, 600)	19.8571	46.3674	(1600, 1800)	19.8571	46.3674	(800, 400)	19.8571	46.8961
(1400, 1000)	19.8571	46.8961	(1400, 1000)	19.8492	46.3674	(1400, 1000)	19.8571	46.8961
(600, 400)	19.8571	39.6423	(1200, 400)	19.8571	39.6423	(1000, 400)	19.8571	46.3674
(600, 200)	19.8571	46.8961	(600, 1800)	19.8571	46.3674	(600, 200)	19.8571	46.3674
(1200, 1800)	19.8492	39.6423	(1200, 1800)	19.8492	39.6423	(1200, 1800)	19.8571	46.3674
(1600, 400)	19.8492	46.3674	(1600, 400)	19.8492	46.3674	(400, 400)	19.8571	46.3674
(1400, 800)	19.8571	39.6423	(1400, 800)	19.8571	39.6423	(1600, 200)	19.8571	46.3674
(1200, 1600)	19.8571	46.3674	(1200, 1600)	19.8571	46.8961	(1200, 1600)	19.8571	46.8961
(1800, 400)	19.8571	46.8961	(1200, 1400)	19.8571	46.8961	(200, 200)	19.8571	39.6423
(1200, 1200)	19.8571	39.6423	(1200, 200)	19.8571	39.6423	(1200, 1400)	19.8571	39.6423
(1400, 400)	19.8571	39.6423	(1400, 400)	19.8571	39.6423	(1200, 400)	19.8571	39.6423
(400, 600)	19.8571	46.3674	(400, 200)	19.8571	46.3674	(800, 200)	19.8571	39.6423

5 Conclusion

The paper proposes an improvement in biogeography based optimization (BBO) based on fitness difference strategy (FD-BBO) and its application in solving the wind farm layout optimization problem with non-uniform hub height and rotor radius. The proposed FD-BBO is shown to be an efficient optimization algorithm by numerical experiments on benchmark test problems. A square wind farm of $2000m \times 2000m$ is taken for numerical experiments of wind farm layout optimization problem. Two cases with 26 turbines and 30 turbines are considered for the experiments. Obtained results are compared with earlier published results and the results obtained by basic BBO and blended BBO. FD-BBO outperforms over all for both the cases. For each case, FD-BBO recommended the single rotor radius which decreases the manufacturer cost of the wind farm. Thus FD-BBO is recommended as reliable and a potential algorithm to solve wind farm layout optimization problem.

6 Acknowledgment

The second author acknowledges the funding from South Asian University, New Delhi, India to carry out this research.

References

[1] G. Mosetti, C. Poloni, B. Diviacco, Optimization of wind turbine positioning in large windfarms by means of a genetic algorithm, Journal of Wind Engineering and Industrial Aerodynamics 51 (1) (1994) 105–116.

[2] S. Grady, M. Hussaini, M. M. Abdullah, Placement of wind turbines using genetic algorithms, Renewable energy 30 (2) (2005) 259–270.

[3] G. Marmidis, S. Lazarou, E. Pyrgioti, Optimal placement of wind turbines in a wind park using monte carlo simulation, Renewable energy 33 (7) (2008) 1455–1460.

[4] J.-F. Herbert-Acero, J.-R. Franco-Acevedo, M. Valenzuela-Rendón, O. Probst-Oleszewski, Linear wind farm layout optimization through computational intelligence, in: Mexican International Conference on Artificial Intelligence, Springer, 2009, pp. 692–703.

[5] N. O. Jensen, A note on wind generator interaction, 1983.

[6] A. Mittal, Optimization of the layout of large wind farms using a genetic algorithm, Ph.D. thesis, Case Western Reserve University (2010).

[7] J. S. González, A. G. G. Rodriguez, J. C. Mora, J. R. Santos, M. B. Payan, Optimization of wind farm turbines layout using an evolutive algorithm, Renewable energy 35 (8) (2010) 1671–1681.

[8] S. Chowdhury, J. Zhang, A. Messac, L. Castillo, Unrestricted wind farm layout optimization (uwflo): Investigating key factors influencing the maximum power generation, Renewable Energy 38 (1) (2012) 16–30.

[9] Y. Chen, H. Li, K. Jin, Q. Song, Wind farm layout optimization using genetic algorithm with different hub height wind turbines, Energy Conversion and Management 70 (2013) 56–65.

[10] J. Park, K. H. Law, Layout optimization for maximizing wind farm power production using sequential convex programming, Applied Energy 151 (2015) 320–334.

[11] K. Chen, M. Song, X. Zhang, S. Wang, Wind turbine layout optimization with multiple hub height wind turbines using greedy algorithm, Renewable Energy 96 (2016) 676–686.

[12] J. C. Bansal, P. Farswan, Wind farm layout using biogeography based optimization, Renewable Energy 107 (2017) 386–402.

[13] X.-S. Yang, S. Deb, Cuckoo search via lévy flights, in: Nature & Biologically Inspired Computing, 2009. NaBIC 2009. World Congress on, IEEE, 2009, pp. 210–214.

[14] S. Rehman, S. Ali, S. Khan, Wind farm layout design using cuckoo search algorithms, Applied Artificial Intelligence (2017) 1–24.

[15] A. Vasel-Be-Hagh, C. L. Archer, Wind farm hub height optimization, Applied Energy 195 (2017) 905–921.

[16] D. Simon, Biogeography-based optimization, Evolutionary Computation, IEEE Transactions on 12 (6) (2008) 702–713.

[17] H. Ma, D. Simon, Blended biogeography-based optimization for constrained optimization, Engineering Applications of Artificial Intelligence 24 (3) (2011) 517–525.

[18] Q. Feng, S. Liu, J. Zhang, G. Yang, L. Yong, Biogeography-based optimization with improved migration operator and self-adaptive clear duplicate operator, Applied Intelligence 41 (2) (2014) 563–581.

[19] G. Xiong, D. Shi, X. Duan, Enhancing the performance of biogeography-based optimization using polyphyletic migration operator and orthogonal learning, Computers & Operations Research 41 (2014) 125–139.

[20] G.-G. Wang, A. H. Gandomi, A. H. Alavi, An effective krill herd algorithm with migration operator in biogeography-based optimization, Applied Mathematical Modelling 38 (9) (2014) 2454–2462.

[21] P. Farswan, J. C. Bansal, Migration in biogeography-based optimization, in: Proceedings of Fourth International Conference on Soft Computing for Problem Solving, Springer, 2015, pp. 385–397.

[22] P. Farswan, J. C. Bansal, K. Deep, A modified biogeography based optimization, in: 2nd International Conference on Harmony Search Algorithm (ICHSA), Korea Univ, Seoul, South Korea: Springer-Verlag Berlin, Springer, 2016, pp. 227–238.

[23] W. Guo, L. Wang, C. Si, Y. Zhang, H. Tian, J. Hu, Novel migration operators of biogeography-based optimization and markov analysis, Soft Computing (2016) 1–28.

[24] M. Lohokare, S. S. Pattnaik, B. K. Panigrahi, S. Das, Accelerated biogeography-based optimization with neighborhood search for optimization, Applied Soft Computing 13 (5) (2013) 2318–2342.

[25] J. C. Bansal, Modified blended migration and polynomial mutation in biogeography-based optimization, Harmony Search Algorithm. Springer (2016) 217–225.

[26] D. Simon, M. G. Omran, M. Clerc, Linearized biogeography-based optimization with re-initialization and local search, Information Sciences 267 (2014) 140–157.

[27] J. C. Bansal, P. Farswan, A novel disruption in biogeography-based optimization with application to optimal power flow problem, Applied Intelligence (2016) 1–26.

[28] J. C. Bansal, H. Sharma, K. Arya, K. Deep, M. Pant, Self-adaptive artificial bee colony, Optimization 63 (10) (2014) 1513–1532.

[29] J. C. Bansal, H. Sharma, S. S. Jadon, M. Clerc, Spider monkey optimization algorithm for numerical optimization, Memetic Computing 6 (1) (2014) 31–47.

[30] S. M. A. Pahnehkolaei, A. Alfi, A. Sadollah, J. H. Kim, Gradient-based water cycle algorithm with evaporation rate applied to chaos suppression, Applied Soft Computing 53 (2017) 420–440.

[31] A. Alireza, Pso with adaptive mutation and inertia weight and its application in parameter estimation of dynamic systems, Acta Automatica Sinica 37 (5) (2011) 541–549.

[32] R. H. MacArthur, E. O. Wilson, The theory of island biogeography, Vol. 1, Princeton University Press, 1967.

[33] M. Clerc, Guided randomness in optimization, Vol. 1, John Wiley & Sons, 2015.

[34] P. N. Suganthan, N. Hansen, J. J. Liang, K. Deb, Y.-P. Chen, A. Auger, S. Tiwari, Problem definitions and evaluation criteria for the cec 2005 special session on real-parameter optimization, KanGAL report 2005005 (2005) 2005.

[35] I. Katic, J. Højstrup, N. O. Jensen, A simple model for cluster efficiency, in: European Wind Energy Association Conference and Exhibition, 1986, pp. 407–410.